Pore closure effect of laser shock peening of additively manufactured AlSi10Mg

Anton du Plessis [a,*], Daniel Glaser [b], Heinrich Moller [c], Ntombizodwa Mathe [b], Lerato Tshabalala [b], Busisiwe Mfusi [d], Roelf Mostert [c]

a. Physics Department, Stellenbosch University, Stellenbosch 7602, South Africa
b. CSIR National Laser Centre, Meiring Naude Road, Brummeria, Pretoria 0001, South Africa
c. Department of Materials Science and Metallurgical Engineering, University of Pretoria, Pretoria 0001, South Africa
d. Chemical, Metallurgical and Materials Engineering Department, Tshwane University of Technology, Staatsartillerie Rd, Pretoria West, Pretoria, 0183

* Corresponding author: anton2@sun.ac.za

This paper reports on an exceptional insight provided by nondestructive X-ray tomography of the same samples before and after laser shock peening. The porosity in two additively manufactured aluminum alloy (AlSi10Mg) tensile samples before and after laser shock peening was imaged using identical X-ray tomography settings and overlap of the data was performed for direct comparison. The results indicate clearly that near-surface pores are closed by the process, while internal pores remain unaffected. Laser shock peening has become well known as a method to improve the fatigue properties of materials, including those of additively manufactured aluminum alloys. This improvement is usually attributed to the compressive residual stress induced by the process. The additional effect of closure of near surface pores that is illustrated in this work is of interest for additive manufacturing because additive manufacturing is not yet able to produce completely pore free components. Since the critical pore initiating fatigue cracks are always attributed to surface or subsurface pores, the closure of these pores may play an additional role in improving the fatigue properties. While more work remains to unravel the relative importance of near-surface porosity compared to the compressive residual stress effect, this work clearly shows the effect of laser shock peening – closing of pores near the surface. For the processing conditions demonstrated here, all pores up to 0.7 mm from the surface are closed without damaging the surface, while higher peening power results in surface damage.

Keywords: additive manufacturing; laser shock peening; aluminum alloys; laser powder bed fusion; X-ray tomography

Preprint submitted to 3D Printing and Additive Manufacturing, July 2019. Final paper available at journal: https://doi.org/10.1089/3dp.2019.0064

1. Introduction

Additive manufacturing has progressed to such an extent that highly dense parts can be produced in various metals, with excellent mechanical properties suitable for critical applications [1,2]. The advances in these processes allow highly complex geometries to be produced for functional applications [3]. However, despite the possibility to produce highly dense parts with appropriate microstructure and surface finish, some micro-porosity may remain and may act as crack initiators in cyclic loading applications. The role of micro-porosity, surface defects and inclusions on fatigue life of metals from all manufacturing processes was initially discussed in [4] and was reviewed recently by the same author [5–7], where the role of each defect type was discussed in relation to fatigue properties. Of particular interest is the observation that surface and subsurface pores are almost always the crack initiation or “killer” pores [8]. A recent study made use of different laser scan parameters to obtain a more dense contour and less dense interior of additively manufactured steel samples and investigated high cycle fatigue – they found that most failures occurred on pores within 0.1 mm of the surface despite much larger and more excessive porosity inside the parts [9].

Due to the potentially detrimental role of manufacturing defects such as porosity on mechanical properties, it has become standard practice to apply hot isostatic pressing (HIPping) to reduce porosity. HIP has been proven to close even very large pores - for example as shown for Ti6Al4V in cast samples - pores of 5 mm diameter were closed entirely [10]. However, in this same work small subsurface pores remained unaffected due presumably to microstructural connection to the surface, making the HIP treatment ineffective for these small subsurface pores. For additively manufactured samples the same surface-connection for layered lack-of-fusion porosity was speculated to explain the ineffective HIP closing of some pores, also in Ti6Al4V [11]. A clustering of excessive numbers of subsurface pores in additively manufactured parts can be caused by different physical processes during the build, including the possibility for mismatch between the contouring and hatching patterns used, or due to slowing of the beam velocity near the edges causing higher energy input leading to keyhole pores. Such subsurface porosity has been reported in a round robin test conducted recently for parts produced in Ti6Al4V [12]. While these studies made use of Ti6Al4V, the processes are similar and applicable to additively manufactured aluminum alloys.

Aluminum holds particular promise for lightweight applications in automotive and aerospace applications as summarized in [13]. Despite its excellent properties, additive manufacturing of aluminum has been a challenge – with large scatter in fatigue results and varying success rates. Uzan et al [14] investigated laser powder bed fusion of AlSi10Mg, and found that heat treatments reduced the strength and fatigue properties of the material. In the work of Brandl et al [15], a large number of samples were analyzed with different build orientations, build platform heating and post-process heat treatment. Good fatigue properties were found despite the presence of pores, but failure always initiated on the pores near or on the surface. In the work of Romano et al [16,17], the fatigue properties were studied in relation to defect distributions for a statistical prediction of fatigue properties. The pores in laser powder bed fusion of AlSi10Mg in one case was reported as containing oxides, which may be trapped in the pore during melting – also here the fatigue initiation was always attributed to the subsurface pores specifically [18]. In the work of Aboulkhair et al [19], process parameters were optimized to minimize process porosity and the best solution was found with a pre-sinter strategy to pass twice over every area – the first time with half the power of the second pass.

Conventional mechanical shot peening (SP) is a cold working process which entails a controlled impingement of solid shot media (such as glass, metallic or ceramic spheres) onto the target workpiece [20]. The impact generates plastic deformation through the surface, and the surrounding material's elastic response is the generation of a compressive stress field. It is known that significant benefits in fatigue crack incubation of aluminum alloys can be induced by shot peening. In general, the mechanism responsible is believed to be related to the introduction of a sub-surface compressive residual stress field. The negative features of accentuated surface roughness and cracking of sub-surface precipitates in the soft and deformable matrix to some extent counter the positive effects of the compressive residual stress induced [21]. When sub-surface pores are introduced, as in the case of parts produced through laser powder bed fusion, fatigue cracks initiate from the pores, negating the compressive residual stress field influence [22]. Tumbling and shot peening was applied to Ti6Al4V samples produced by laser powder bed fusion and improved fatigue properties were reported for shot peened samples [23]. For AlSi10Mg produced by laser powder bed fusion, a comparison of shot peened and un-peened samples showed the fatigue crack initiation site to be from deeper in the sample for shot peened samples, coupled with an improvement in fatigue life [24].

For AlSi10Mg alloys, mechanical shot peening has been shown to result in pore shrinkage in the sub-surface region (0 – 500 micron), imaged using X-ray tomography [25]. An improvement in the depth of the residual stress zone but not the peak compressive stress value was also observed [25]. Since most of the fatigue cracks in the untreated sample originated in the 0 – 200 micron zone, it was unclear if the deepening of the compressive residual stress zone or the pore size reduction was primarily responsible for the low-cycle and high-cycle fatigue improvements observed in that case (33% increase in fatigue limit, 4 – 6 times increase in low-cycle fatigue life).

The study of the influence of laser shock peening (LSP) on the distribution of sub-surface pores in laser powder bed fusion parts therefore clearly warrants investigation. LSP has the potential benefits of shot peening in reducing porosity, as well as introducing a compressive stress field [26–28], without the negative aspects of shot peening, namely increasing surface roughness and leading to cracking of precipitates in relatively soft aluminum alloys. Some work has recently been done regarding the effect of LSP on aluminum alloys [29], but the investigations focused mainly on the effects on weldments. A combination of LSP and laser powder bed fusion in the same process was recently also proposed which shows some promise [30]. LSP of additive manufactured metals has been demonstrated and proven to be an effective post-processing tool for improving fatigue properties [31,32].

Despite the evidence of porosity reduction both by shot peening as well as laser shock peening, evidence of the pore-closure effect of LSP remains lacking. The present paper reports such evidence with exceptional detail and shows surprising pore-closing efficiency, quantifying the depth to which this occurs.

2. Materials and methods

Samples were produced out of AlSi10Mg alloy using the SLM 280 2.0 (SLM Solutions) laser powder bed fusion system with standard processing parameters for AlSi10Mg as prescribed by the manufacturer, including 370 W, 30 micron layer thickness, 1000 mm/s scan speed and 0.19 mm hatch spacing. Powder from SLM solutions was used, with mean particle size 40 µm. Stress relief heat treatment was performed after the build at 300 degrees for 2 hours. Two samples were produced for tensile testing with cylindrical hourglass geometry and gauge diameter of 5 mm. One sample was built in a horizontal orientation and one in a vertical orientation relative to baseplate, with a stress relief heat treatment performed prior to removal from the baseplate. No further surface or heat treatments were employed, and the samples were therefore used in the stress-relieved condition with rough surfaces. For optical microscopy, one sample was sectioned near the centre, polished and then etched.

The LSP processing was performed at the CSIR National Laser Centre (Pretoria, South Africa) on a processing platform developed in-house. The platform was specifically devised for R&D in aerospace and power generation applications [33,34]. The work-cell incorporates an Nd:YAG laser operating at a 532 nm wavelength with a 5.1 ns pulse duration. A 1.5 mm round laser spot is achieved on the target, with a thin water layer applied with a spray nozzle to provide inertial confinement. The energy of the laser pulses was attenuated to achieve power intensities of 5 and 10 GW/cm^2 on the target surface in the direct ablation mode (i.e. Laser Peening without a protective coating). For LSP processing, power is often regarded as the dominant parameter as this can be directly related to the magnitude of the pressure pulse developed according to the relationship described in [27]. In this configuration, the expected shock pressures are 4 and 7 GPa for 5 and 10 GW/cm^2 respectively. In order to process a sample area using the 1.5 mm spot size, an overlap strategy is employed whereby sequential shots are overlapped with equal displacement in the vertical and horizontal direction. A pulse density of 5 spots per mm^2, which equates to 70.2% overlap between spot centers, is used.

MicroCT was performed at the Stellenbosch CT facility [35] using 150 kV and 130 µA, with 20 µm voxel size. This means that only pores larger than 20 µm are visible in CT slice images, and pores larger than 60 µm are quantitatively evaluated (3x3x3 voxels in extent). This was performed under identical conditions before and after laser shock peening. Image analysis was performed in VGSTUDIO MAX 3.2. The use of microCT for imaging porosity in additive manufacturing, especially before and after processing steps, was outlined in a recent review paper [36]. The samples contained dense particles due to contamination from a previous build. In the present study, this helped with the precise alignment of before-after scan data, and to further confirm that the observed closure is not due to sample misalignment or deformation.

3. Results and discussion

The microCT scan results from before and after laser shock peening at 5 GW/cm^2 of the vertical-built sample are presented in three selected and carefully aligned microCT slice views in Figure 1. All near-surface pores are entirely closed below the resolution limit, while internal pores are unaffected. These unaffected pores in the center of the sample confirm the ability to detect pores, while the inclusions allow precise alignment, thus validating the lack of pores near the surface. Dimensional measurements show that a pore at 0.38 mm from the surface is entirely closed (or reduced down to below the scan resolution of 0.02 mm) while an internal pore at a distance of 0.84 mm from the surface is unaffected. The gauge diameter in this case is 4.81 mm. Figure 2 shows the central 10 mm section of the same sample before and after LSP with a 3D porosity analysis, clearly indicating porosity reduction and in particular that all subsurface pores are closed (when viewed from top). Figure 3 shows quantitative analysis of porosity for the 10 mm central section with number of pores plotted against their distance from the surface. This clearly shows that no pores remain within 0.7 mm from the surface. This is a significantly stronger effect of pore closure as compared to mechanical shot peening where similar tests showed only pore shrinkage [25]. Despite the clear evidence provided, it is possible that only shrinkage occurred and that final pore sizes are simply below the detection limit of the scan (0.02 mm). The initial pore sizes are roughly 0.1 mm, ranging from 0.06 to 0.25 mm in the scan before LSP. If a 0.1 mm pore is closed to below 0.02 mm, this indicates a shrinkage or closure of at least 80 %, which is significantly higher than the shrinkage reported for shot peening in the study mentioned above.

Preprint submitted to 3D Printing and Additive Manufacturing, July 2019. Final paper available at journal: https://doi.org/10.1089/3dp.2019.0064

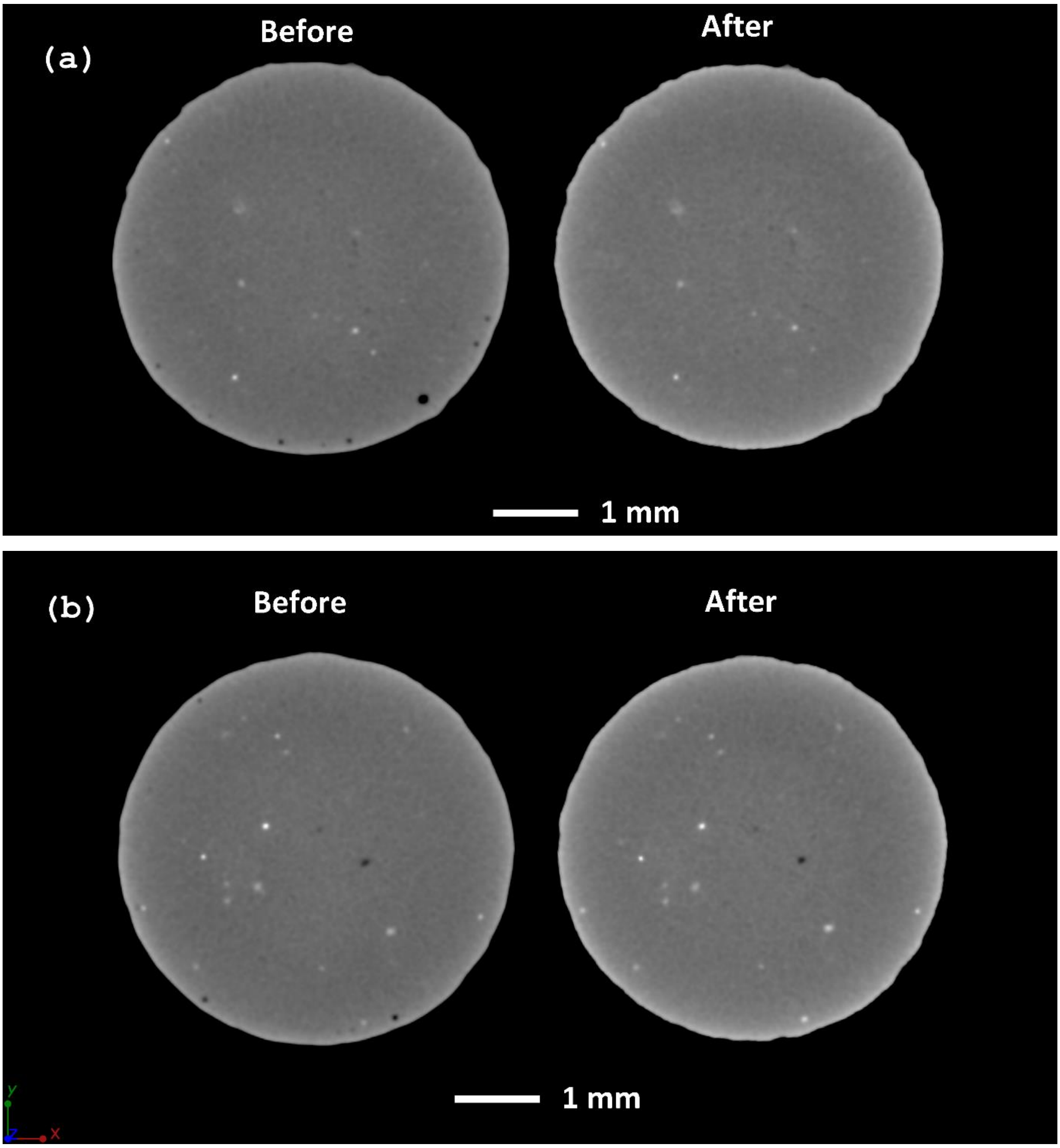
(a)
Before
After
1 mm
(b)
Before
After
1 mm
y
z
x

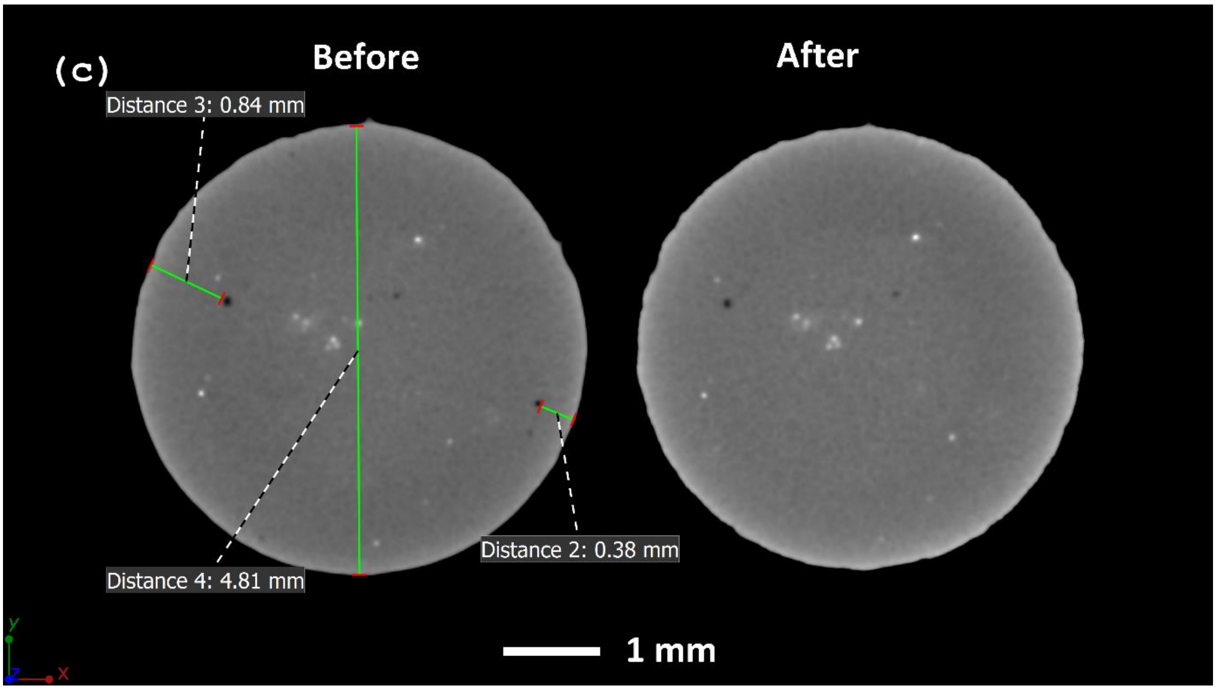

Figure 1: Before (left) and after (right) the laser shock peening. Three selected cross-sectional microCT slice images (top view) of vertical-built sample, with near surface pores which disappear due to peening. Inclusions assist in validating the alignment of the before-after scan data. (a) and (b) show different slice views and (c) shows selected measurements.

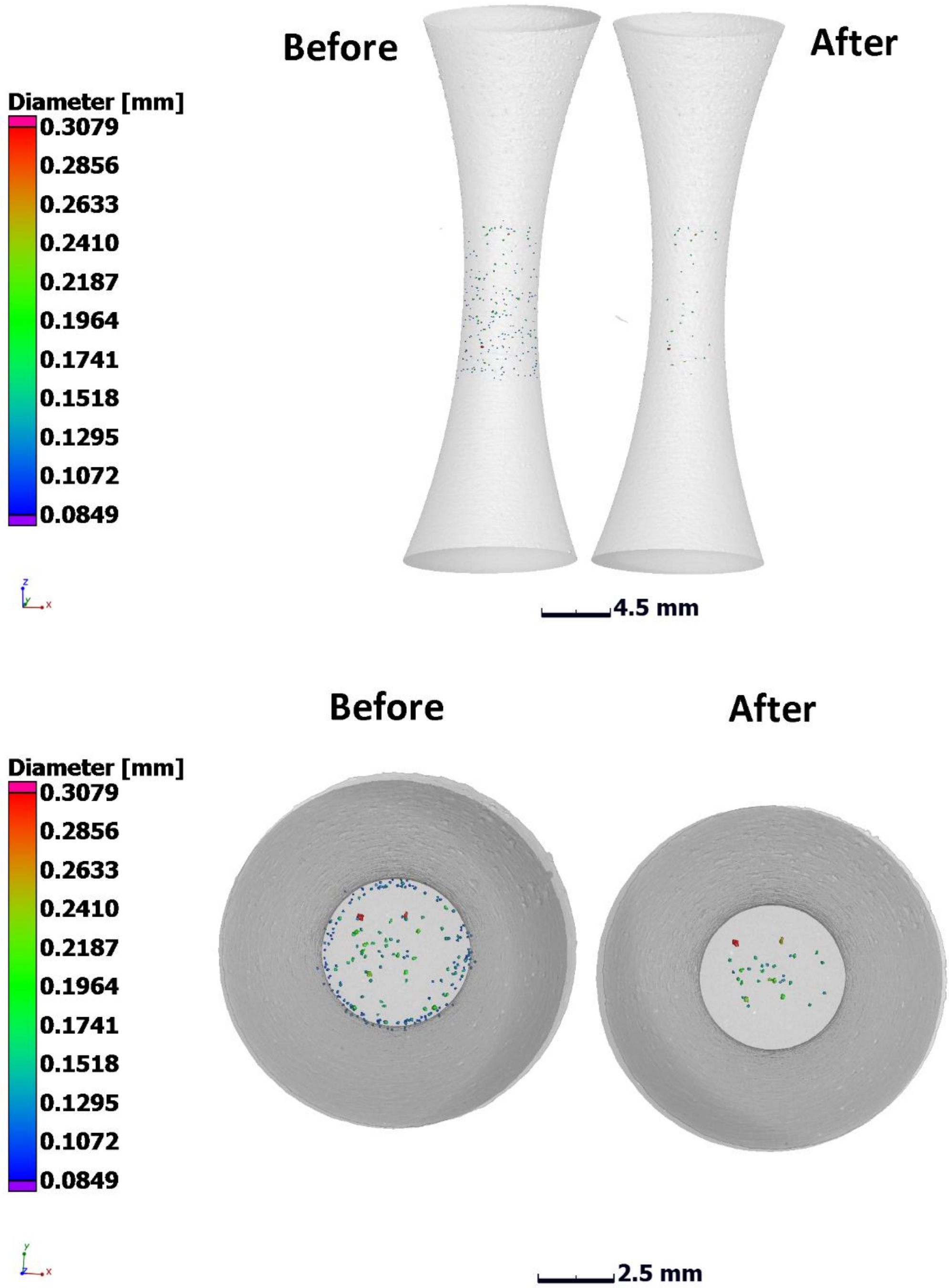

Figure 2: 3D visualizations of porosity in the central 10 mm of the gauge section before (left) and after peening (right). This clearly shows the reduction of porosity, especially for the near-surface pores, shown in (a) front and (b) top views.

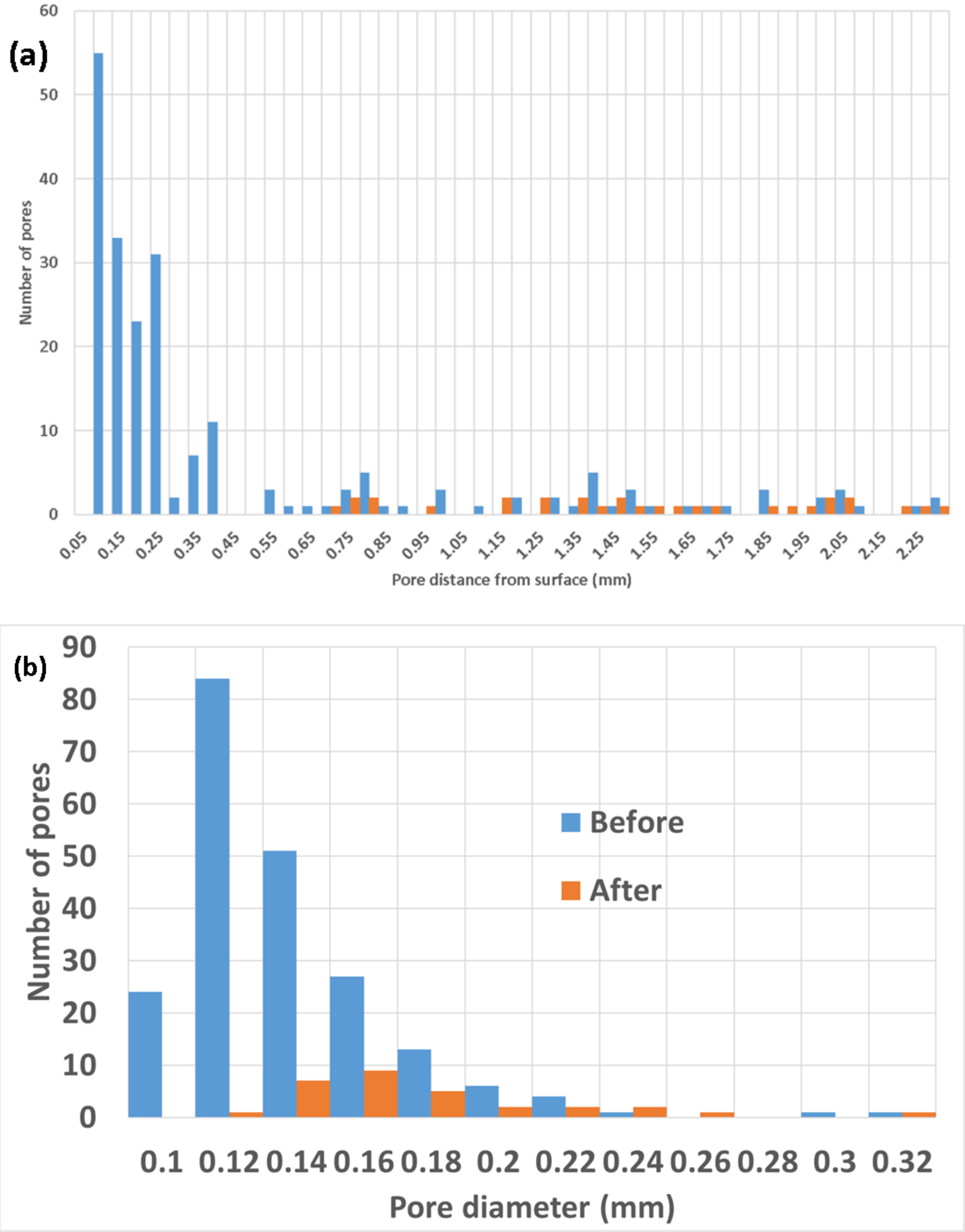

Figure 3: (a) shows pore number vs distance from surface in the central 10 mm of the gauge section – before and after peening. No pores are detected within 0.7 mm from the surface post-peening. (b) shows pore number as function of pore diameter before and after peening.

As an approximation to illustrate the beneficial effect on fatigue properties, a simple calculation of stress intensity factor for each pore before and after laser shock peening was performed. This was done for the hourglass-shaped sample subjected to bending-fatigue using relationships found in Murakami [4] and using defect information from the defect analysis data for each state. The result is shown in Figure 4, which indicates that before peening, many pores had high stress intensity factors, while few of these remain after peening.

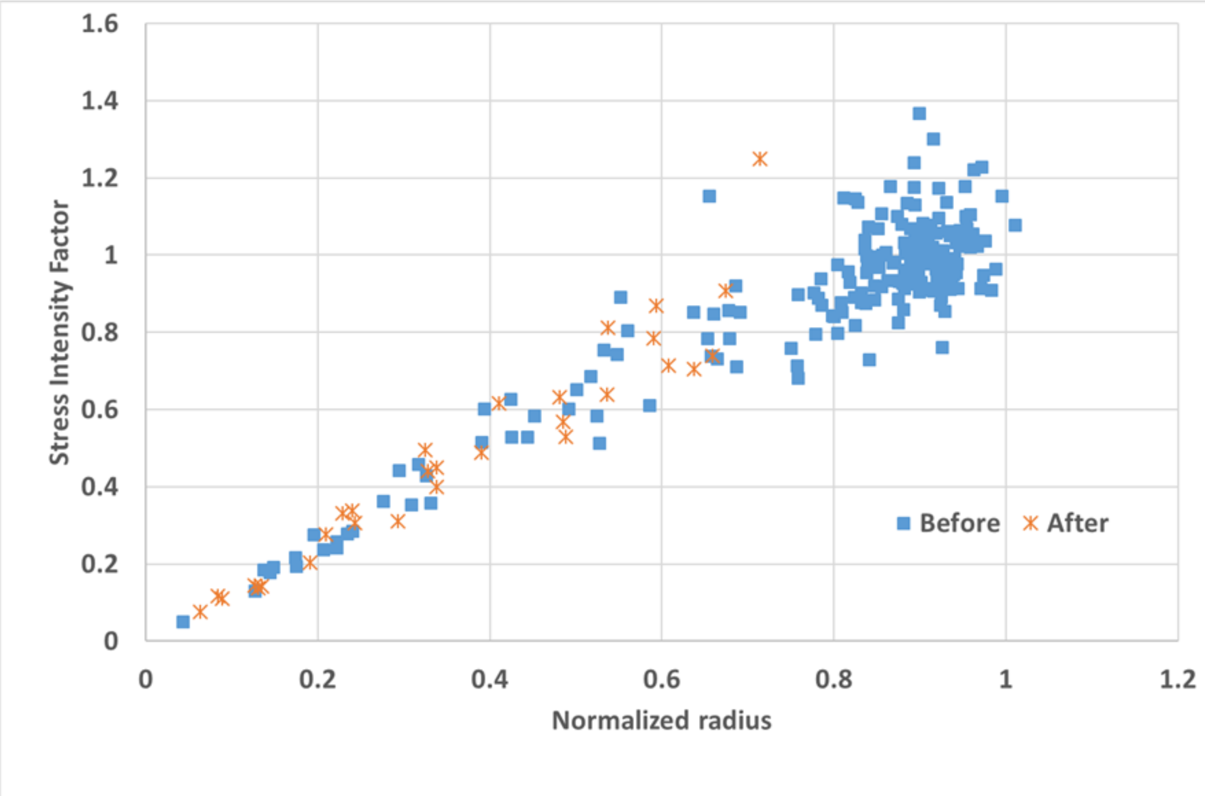

Figure 4: Stress intensity factor calculated from defect data before and after laser shock peening – for bending fatigue.

For the system configuration utilized, typically no more than 5 GW/cm^2 is necessary to process high strength aluminum alloys such as AA7075 and AA7050. The peening parameter of 5 GW/cm^2 (as used for the vertical-built sample) is therefore considered high for the current application, but the results show no surface damage and significant pore closure. The use of the 10 GW/cm^2 which was used for the horizontally built sample is expected to be excessive and can potentially cause surface degradation. This horizontal sample had a rougher surface initially due to the down-skin irregular surface with support structures removed, without any further machining or smoothing. This additional roughness may contribute to problems in applying the LSP process properly. Despite the initially rough surface, peening was applied successfully. As expected from the high power settings used, this sample did indeed have surface damage additionally induced by over-peening as seen in Figure 5. This indicates

Preprint submitted to 3D Printing and Additive Manufacturing, July 2019. Final paper available at journal: https://doi.org/10.1089/3dp.2019.0064

the need to optimize peening parameters and investigate the damage that can be caused, particularly when applied to surfaces of varying roughness. Despite the surface damage and rough initial surface, pore closure is again observed as seen by the slice image in Figure 5.

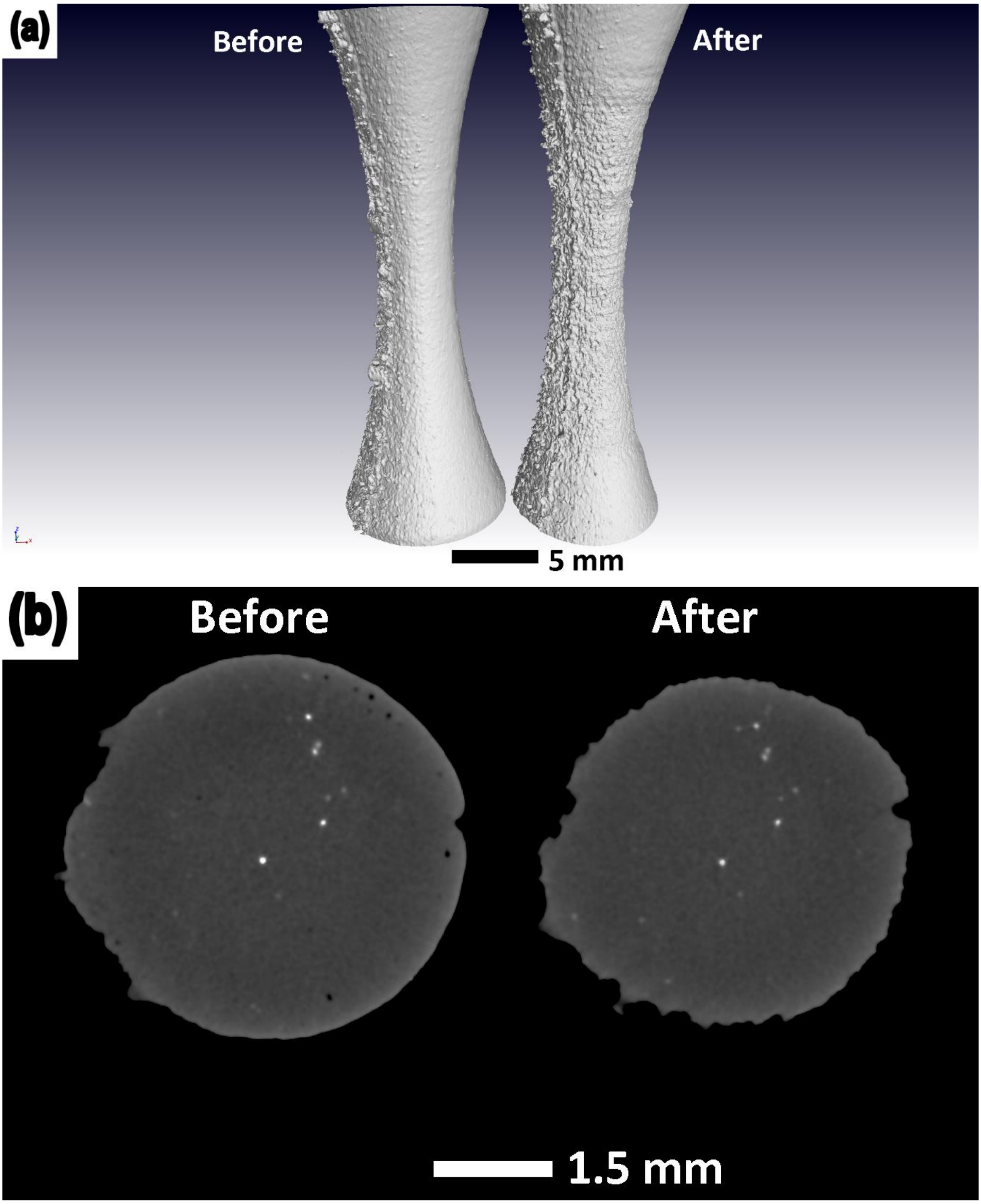

Figure 5: Damaging effect of peening when laser peening power too high, though pore closure effect still observed. (a) 3D surface view before (left) and after (right) peening showing increased surface roughness in post-peening state. (b) Slice images in center of gauge length viewed from top, indicating before (left) and after (right) peening – pore closure and surface modification observed.

Preprint submitted to 3D Printing and Additive Manufacturing, July 2019. Final paper available at journal: https://doi.org/10.1089/3dp.2019.0064

The vertical specimen (Figures 1-3) was further sectioned for optical microscopy and Figure 6 shows cross-sectional views in a top view orientation (viewed in build direction of sample). Samples were polished and etched, but it must be noted that excessive polishing of aluminum closes pores and some preparation flaws are present here. There is a clear region indicated by the blue line which correspond to the contour-track region were few pores are seen. White arrows indicate large pores on the inside of the sample. A clear border between contour and hatch regions, which caused a preparation flaw during etching is visible. What is clear is that less pores are present near the surface as compared to inside the sample, but some pores are present within the 0.7 mm region close to the surface which are missed by the X-ray tomography results, as these are smaller than the scan resolution. The closure efficiency (or degree of closure) is therefore dependent on the distance from the surface.

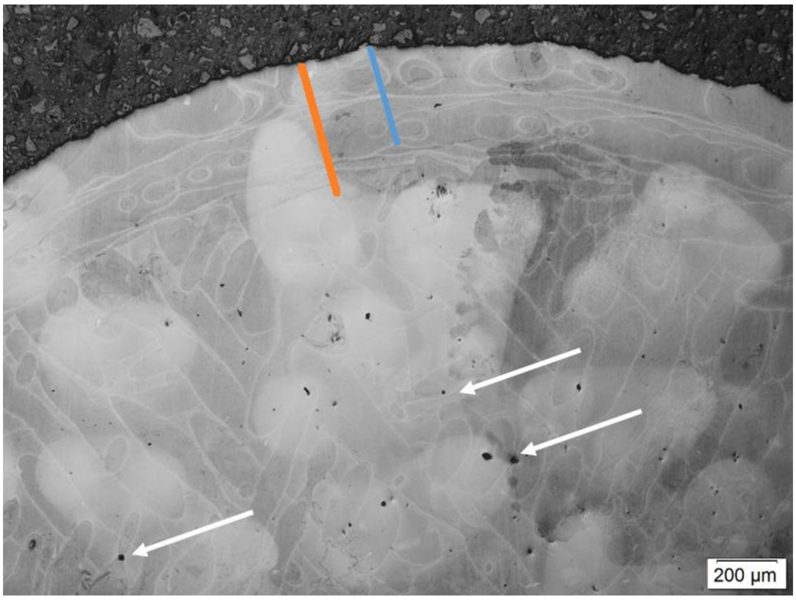

Figure 6: Optical microscopy showing internal pores (white arrows), depth to which pore closure is observed (~0.7 mm, orange line) and shorter blue line indicating contour scan track region. .

4. Conclusions

We demonstrate clear evidence of the pore-closing effect of laser shock peening. This result can partly explain the positive effect the technique has on fatigue properties of parts, as surface pores are often found to be crack initiation sites in fatigue tests. This is an area which has not been studied widely since the compressive residual stress induced is widely assumed to be the largest contributing factor to improved fatigue life. Considering the small size of pores found in additively manufactured materials, the fact that subsurface pores are almost always the fatigue crack initiating defect, and the fact that other processing techniques may cause damage to the surface or not be effective for near-

Preprint submitted to 3D Printing and Additive Manufacturing, July 2019. Final paper available at journal: https://doi.org/10.1089/3dp.2019.0064

surface pores, these results are considered extremely important and may be a viable alternative to improving the mechanical properties of critical components. This has wide implications for the improvement of properties of especially additively manufactured parts, but also parts produced by other techniques. The effect is most likely not limited to aluminum alloys.

Acknowledgements

The South African Department of Science and Technology is acknowledged for support through the Collaborative Program for Additive Manufacturing (CPAM). Stephan le Roux is acknowledged for technical assistance.

References

[1] T. Debroy, H.L. Wei, J.S. Zuback, T. Mukherjee, J.W. Elmer, J.O. Milewski, A.M. Beese, A. Wilson-Heid, A. De, W. Zhang, Additive manufacturing of metallic components – Process, structure and properties, Prog. Mater. Sci. 92 (2018) 112–224. doi:10.1016/j.pmatsci.2017.10.001.

[2] D. Bourell, J.P. Kruth, M. Leu, G. Levy, D. Rosen, A.M. Beese, A. Clare, Materials for additive manufacturing, CIRP Ann. 66 (2017) 659–681. doi:10.1016/J.CIRP.2017.05.009.

[3] A. du Plessis, C. Broeckhoven, I. Yadroitsava, I. Yadroitsev, C.H. Hands, R. Kunju, D. Bhate, Beautiful and Functional: A Review of Biomimetic Design in Additive Manufacturing, Addit. Manuf. (2019). doi:10.1016/J.ADDMA.2019.03.033.

[4] Y. Murakami, Metal fatigue: effects of small defects and nonmetallic inclusions, Elsevier, 2002.

[5] U. Zerbst, M. Madia, C. Klinger, D. Bettge, Y. Murakami, Defects as a root cause of fatigue failure of metallic components. I: Basic aspects, Eng. Fail. Anal. 97 (2019) 777–792. doi:10.1016/j.engfailanal.2019.01.055.

[6] U. Zerbst, M. Madia, C. Klinger, D. Bettge, Y. Murakami, Defects as a root cause of fatigue failure of metallic components. II: Non-metallic inclusions, Eng. Fail. Anal. (2019) 1–12. doi:10.1016/j.engfailanal.2019.01.054.

[7] Y. Murakami, C. Klinger, M. Madia, U. Zerbst, D. Bettge, Defects as a root cause of fatigue failure of metallic components. III: Cavities, dents, corrosion pits, scratches, Eng. Fail. Anal. 97 (2019) 759–776. doi:10.1016/j.engfailanal.2019.01.034.

[8] L.B. Malefane, W.B. Du Preez, M. Maringa, A. Du Plessis, Tensile and high cycle fatigue

properties of annealed Ti6Al4V (ELI) specimens produced by direct metal laser sintering, South African J. Ind. Eng. 29 (2018) 299–311. doi:10.7166/29-3-2077.

[9] O. Andreau, E. Pessard, I. Koutiri, J.D. Penot, C. Dupuy, N. Saintier, P. Peyre, A competition between the contour and hatching zones on the high cycle fatigue behaviour of a 316L stainless steel: Analyzed using X-ray computed tomography, Mater. Sci. Eng. A. 757 (2019) 146–159. doi:10.1016/j.msea.2019.04.101.

[10] A. du Plessis, P. Rossouw, Investigation of Porosity Changes in Cast Ti6Al4V Rods After Hot Isostatic Pressing, J. Mater. Eng. Perform. (2015). doi:10.1007/s11665-015-1580-4.

[11] A. Du Plessis, S.G. Le Roux, J. Els, G. Booysen, D.C. Blaine, Application of microCT to the non-destructive testing of an additive manufactured titanium component, Case Stud. Nondestruct. Test. Eval. 4 (2015) 1–7. doi:10.1016/j.csndt.2015.09.001.

[12] A. du Plessis, S.G. le Roux, Standardized X-ray tomography testing of additively manufactured parts: a round robin test, Addit. Manuf. (2018). doi:10.1016/J.ADDMA.2018.09.014.

[13] D. Buchbinder, H. Schleifenbaum, S. Heidrich, W. Meiners, J. Bültmann, High Power Selective Laser Melting (HP SLM) of Aluminum Parts, Phys. Procedia. 12 (2011) 271–278. doi:10.1016/J.PHPRO.2011.03.035.

[14] N.E. Uzan, R. Shneck, O. Yeheskel, N. Frage, Fatigue of AlSi10Mg specimens fabricated by additive manufacturing selective laser melting (AM-SLM), Mater. Sci. Eng. A. 704 (2017) 229–237. doi:10.1016/j.msea.2017.08.027.

[15] E. Brandl, U. Heckenberger, V. Holzinger, D. Buchbinder, Additive manufactured AlSi10Mg samples using Selective Laser Melting (SLM): Microstructure, high cycle fatigue, and fracture behavior, Mater. Des. 34 (2012) 159–169. doi:10.1016/j.matdes.2011.07.067.

[16] S. Romano, A. Brückner-Foit, A. Brandão, J. Gumpinger, T. Ghidini, S. Beretta, Fatigue properties of AlSi10Mg obtained by additive manufacturing: Defect-based modelling and prediction of fatigue strength, Eng. Fract. Mech. (2017). doi:10.1016/J.ENGFRACMECH.2017.11.002.

[17] S. Romano, A. Brandão, J. Gumpinger, M. Gschweitl, S. Beretta, Qualification of AM parts: Extreme value statistics applied to tomographic measurements, Mater. Des. 131 (2017) 32–48. doi:10.1016/j.matdes.2017.05.091.

[18] M. Tang, P.C. Pistorius, Oxides, porosity and fatigue performance of AlSi10Mg parts produced by selective laser melting, Int. J. Fatigue. 94 (2017) 192–201. doi:10.1016/j.ijfatigue.2016.06.002.

[19] N.T. Aboulkhair, N.M. Everitt, I. Ashcroft, C. Tuck, Reducing porosity in AlSi10Mg parts processed by selective laser melting, Addit. Manuf. 1–4 (2014) 77–86. doi:10.1016/J.ADDMA.2014.08.001.

[20] M.K. Kulekci, U. Esme, Critical analysis of processes and apparatus for industrial surface peening technologies, Int. J. Adv. Manuf. Technol. 74 (2014) 1551–1565. doi:10.1007/s00170-014-6088-9.

[21] D.J. Chadwick, S. Ghanbari, D.F. Bahr, M.D. Sangid, Crack incubation in shot peened AA7050 and mechanism for fatigue enhancement, Fatigue Fract. Eng. Mater. Struct. 41 (2018) 71–83. doi:10.1111/ffe.12652.

[22] H. Toda, S. Masuda, R. Batres, M. Kobayashi, S. Aoyama, M. Onodera, R. Furusawa, K. Uesugi, A. Takeuchi, Y. Suzuki, Statistical assessment of fatigue crack initiation from sub-surface hydrogen micropores in high-quality die-cast aluminum, Acta Mater. 59 (2011) 4990–4998. doi:10.1016/j.actamat.2011.04.049.

[23] L. Denti, E. Bassoli, A. Gatto, E. Santecchia, P. Mengucci, Fatigue life and microstructure of additive manufactured Ti6Al4V after different finishing processes, Mater. Sci. Eng. A. 755 (2019) 1–9. doi:10.1016/j.msea.2019.03.119.

[24] N.E. Uzan, S. Ramati, R. Shneck, N. Frage, O. Yeheskel, On the effect of shot-peening on fatigue resistance of AlSi10Mg specimens fabricated by additive manufacturing using selective laser melting (AM-SLM), Addit. Manuf. 21 (2018) 458–464. doi:10.1016/j.addma.2018.03.030.

[25] J. Damon, S. Dietrich, F. Vollert, J. Gibmeier, V. Schulze, Process dependent porosity and the influence of shot peening on porosity morphology regarding selective laser melted AlSi10Mg parts, Addit. Manuf. 20 (2018) 77–89. doi:10.1016/J.ADDMA.2018.01.001.

[26] C.S. Montross, T. Wei, L. Ye, G. Clark, Y.W. Mai, Laser shock processing and its effects on microstructure and properties of metal alloys: A review, Int. J. Fatigue. 24 (2002) 1021–1036. doi:10.1016/S0142-1123(02)00022-1.

[27] R. Fabbro, P. Peyre, L. Berthe, X. Scherpereel, Physics and applications of laser-shock processing, J. Laser Appl. 10 (1998) 265–279. doi:10.2351/1.521861.

[28] P. Payre, R. Fabbro, Laser shock processing : a review of the physics and applications, Opt. Quantum Electron. 27 (1995) 1213–1229. doi:10.1007/BF00326477.

[29] G. Sun, X. Fang, Z. Tong, Z. Ni, Y. Lu, Effect of laser shock peening on aluminium alloy laser-welds, Surf. Eng. 32 (2016) 943–948. doi:10.1080/02670844.2016.1194513.

[30] N. Kalentics, E. Boillat, P. Peyre, C. Gorny, C. Kenel, C. Leinenbach, J. Jhabvala, R.E. Logé, 3D Laser Shock Peening – A new method for the 3D control of residual stresses in Selective Laser Melting, Mater. Des. 130 (2017) 350–356. doi:10.1016/j.matdes.2017.05.083.

[31] L. Hackel, J.R. Rankin, A. Rubenchik, W.E. King, M. Matthews, Laser peening: A tool for additive manufacturing post-processing, Addit. Manuf. 24 (2018) 67–75. doi:10.1016/j.addma.2018.09.013.

[32] D. Glaser, S. van Staden, N. Ivanovic, C. Polese, The potential enhancement of components produced by metal additive manufacturing using laser shock processing, in: Proc. RAPDASA, RAPDASA, 2017: pp. 1–15.

[33] D. Glaser, C. Polese, R.D. Bedekar, J. Plaisier, S. Pityana, B. Masina, T. Mathebula, E. Troiani, Laser Shock Peening on a 6056-T4 Aluminium Alloy for Airframe Applications, Adv. Mater. Res. 891–892 (2014) 974–979. doi:10.4028/www.scientific.net/amr.891-892.974.

[34] M. Newby, A. Steuwer, D. Glaser, C. Polese, D. Hattingh, C. Gorny, Synchrotron XRD Evaluation of Residual Stresses Introduced by Laser Shock Peening for Steam Turbine Blade Applications, Mater. Res. Proc. 4 (2018) 97–102. doi:http://dx.doi.org/10.21741/9781945291678-15.

[35] A. du Plessis, S.G. le Roux, A. Guelpa, The CT Scanner Facility at Stellenbosch University: An open access X-ray computed tomography laboratory, Nucl. Instruments Methods Phys. Res. Sect. B Beam Interact. with Mater. Atoms. 384 (2016) 42–49. doi:10.1016/J.NIMB.2016.08.005.

[36] A. du Plessis, I. Yadroitsev, I. Yadroitsava, S.G. Le Roux, X-Ray Microcomputed Tomography in Additive Manufacturing: A Review of the Current Technology and Applications, 3D Print. Addit. Manuf. 5 (2018) 3dp.2018.0060. doi:10.1089/3dp.2018.0060.

Preprint submitted to 3D Printing and Additive Manufacturing, July 2019. Final paper available at journal: https://doi.org/10.1089/3dp.2019.0064